

## Rheological properties of aerosol foams containing aqueous cationic polymer and anionic surfactant

YOSHIFUMI YAMAGATA, *Material Science Research Center, Lion Corporation, 7-13-12 Hirai, Edogawa-ku, Tokyo 132-0035, Japan.*

*Accepted for publication September 30, 1999.*

### Synopsis

Aerosol foams containing cationic cellulose of different molecular weights and an anionic surfactant were studied by using the cyclic shearing tests. The yield value,  $\tau_B$ , of the aerosol foams increased with the apparent viscosity of the concentrate,  $\eta_c$ . However, the apparent viscosity of the foam,  $\eta_f$ , showed a maximum value when plotted against  $\eta_c$  at the charge ratio between the cationic cellulose and the anionic surfactant,  $R_{max}$ , between 2.0 and 4.0. From these results, we presume that the dissolved states for the polymer and the surfactant in the liquid film of the foam are different below and above  $R_{max}$ .

### INTRODUCTION

Foam can be produced by various methods. By an air injection method, air is blown into the vessel containing a surfactant solution. Shaking, rotating, and stirring methods are also applicable (1). In other methods, liquefied hydrocarbon gases are allowed to evaporate and serve as foaming agents or as a propellant. The foam generated by this method is called aerosol foam, and is used as shaving and styling foams in the field of cosmetics. The above-mentioned foams were so unstable hitherto that it was difficult to study them experimentally.

There are several factors associated with foam instability, i.e., drainage rupture of the liquid films followed by coalescence, and change in bubble size (2). To improve stability, multiple surfactants (2,3) or water-soluble polymers (4) are added. It is known that foam properties are considerably affected by complexes formed by the addition of long-chain alcohols to ionic surfactants in an aqueous solution, as a result of being adsorbed at the air/liquid interface (2,3,5).

Another complex has been investigated for the system using water-soluble polymers with ionic surfactants (6–11). For example, Goddard and co-workers (6–8,12–19) and Ohbu *et al.* (20,21) studied complex formation between water-soluble cationic cellulose polymers and anionic or amphoteric surfactants. It is generally accepted that the formation and precipitation of the complex formed between polyelectrolytes and oppositely charged surfactants and the resolubilization by excess surfactants are due to the simultaneous electrostatic and hydrophobic interactions between them.

However, few foam systems have been reported in which the complex between a water-soluble cationic polymer and an anionic surfactant were combined. In the present paper, we examine systematically the rheological properties of the foams prepared from a glycidyl trimethylammonium chloride, adduct to hydroxyethylcellulose and an anionic acyl glutamate. We discuss the dissolved states of the components in foams on the basis of macroscopic flow behavior, together with direct microscopic observation of the foam.

## EXPERIMENTAL

### MATERIALS

Cationic celluloses of different molecular weights (cationic cellulose, Leogard<sup>®</sup>, Lion Corp.), were used as water-soluble cationic polymers. Figure 1 shows the structural formula of the cationic celluloses of molecular weight 50,000, 150,000, or 500,000, identified as L-type, M-type, and H-type, respectively. The average degree of cationic substitution was about 0.3–0.4 per anhydroglucose unit. A surfactant used was triethanolamine cocoyl-l-glutamate (Amisoft<sup>®</sup> CT-12, Ajinomoto Corp.). The nonionic surfactant nonoxynol-15 (Liponox<sup>®</sup> NC-150, Lion Corp.) was also used in the solubilized system. All compounds were used without further purification.

Aqueous solutions, described as concentrates, were prepared by adding 0.1 wt% anionic surfactant, 0.5 wt% nonionic surfactant, and various amounts of the cationic celluloses to deionized water, and mixing and stirring with a rod with four paddles at room temperature. The prepared concentrates (94 parts and six parts of a propellant [w/w]) were confined in a pressure-proof aluminum container (35-mm diameter). The propellant used was liquefied petroleum gas consisting of propane, n-butane, and isopentane with an equilibrium vapor pressure of  $4.4 \times 10^5$  Pa at 20°C.

### MEASUREMENT

All experiments were carried out at 25°C. When the aluminum container was allowed to stand, the contents were separated into two layers, i.e., concentrate and propellant phases. In such a condition, uniform foam cannot be obtained even if the contents are

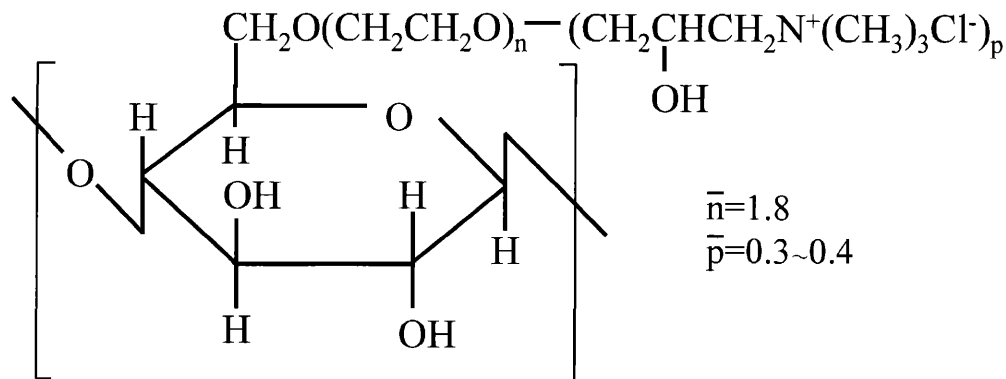


Figure 1. Structural formula of cationic cellulose.

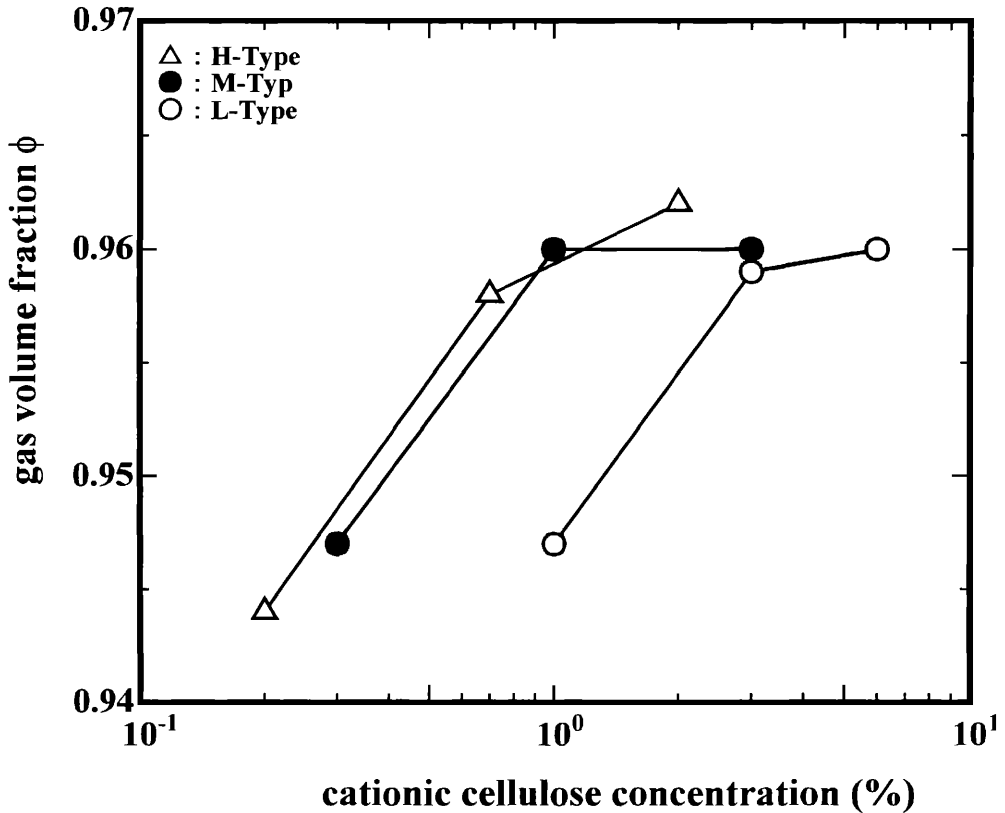


Figure 2. Relationship between gas volume fraction ( $\phi$ ) and cationic cellulose concentration.

sprayed out. Therefore, the container was shaken ten times by hand before each measurement to emulsify the concentrate and the propellant.

A tube (*ca.* 2-mm diameter and 50-mm length) was attached at the top of the spout. Aerosol foam was carefully filled into an empty cylindrical vessel of volume  $V_0$  (54.46 cm<sup>3</sup>), and the density of the foam was calculated from the weight difference between the empty vessel,  $W_0$ , and the filled one,  $W$ . Thus, the gas volume fraction,  $\phi$ , could be obtained from equation 1:

$$\phi = 1 - (W - W_0)/V_0 \quad (\text{Eq. 1})$$

The bubble structure of the aerosol foams was observed using an optical microscope. An average bubble size ( $D_N$ ) was calculated from the number of bubbles,  $N$ , per unit area, using equation 2:

$$D_N = \sqrt{\frac{A}{N\pi}} \quad (\mu\text{m}) \quad (\text{Eq. 2})$$

The concentrates and the aerosol foams were subjected to rheometry using an MR-3 rheometer (Rheology Engineering). Flow curves in periodical shear experiments were taken with a concentric-cylinder setup for the concentrates and a cone-plate setup for the

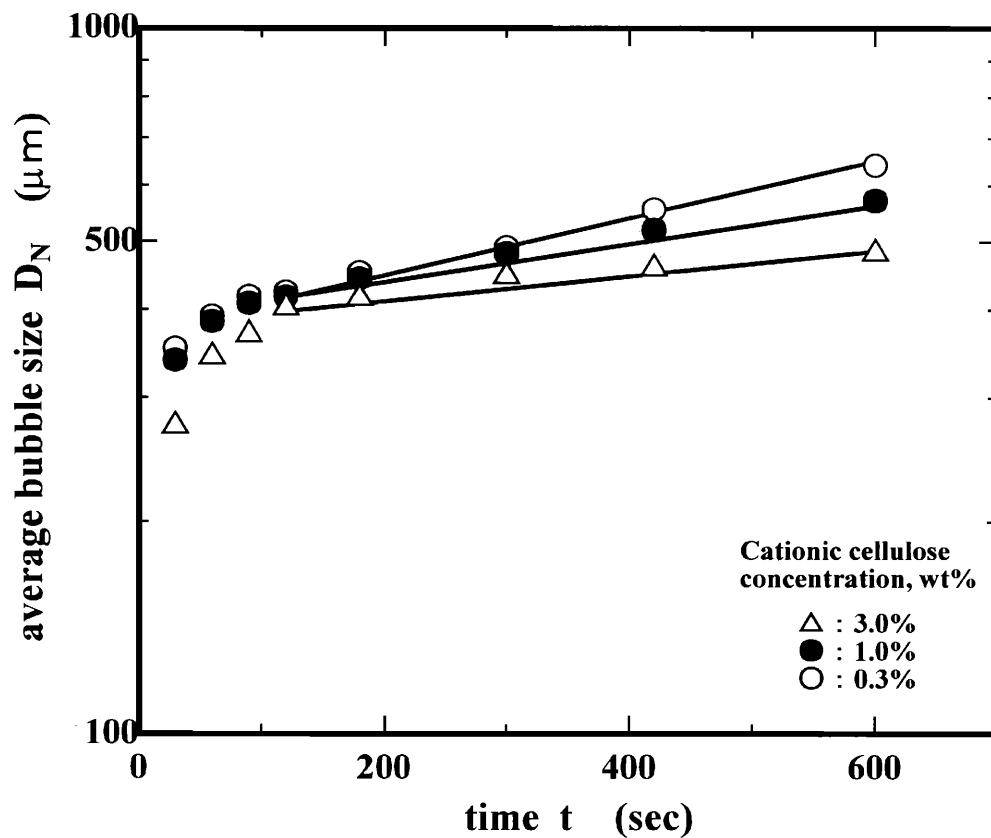


Figure 3. Change in the average bubble size ( $D_N$ ) on aging (M-type).

Table I  
Relationship Between Bubble Size ( $D_0$ ), Rate Constant of Coalescence ( $k$ ), and Cationic Cellulose Concentration

Cationic cellulose			
Type	Wt%	$D_0$ ( $\mu\text{m}$ )	$k$ ( $\times 10^{-4}$ $\text{sec}^{-1}$ )
L	1.0	382	13.2
	3.0	395	7.2
	6.0	403	3.9
M	0.3	385	8.5
	1.0	389	6.6
	3.0	390	3.7
H	0.2	336	13.0
	0.7	342	6.9
	2.0	341	4.6

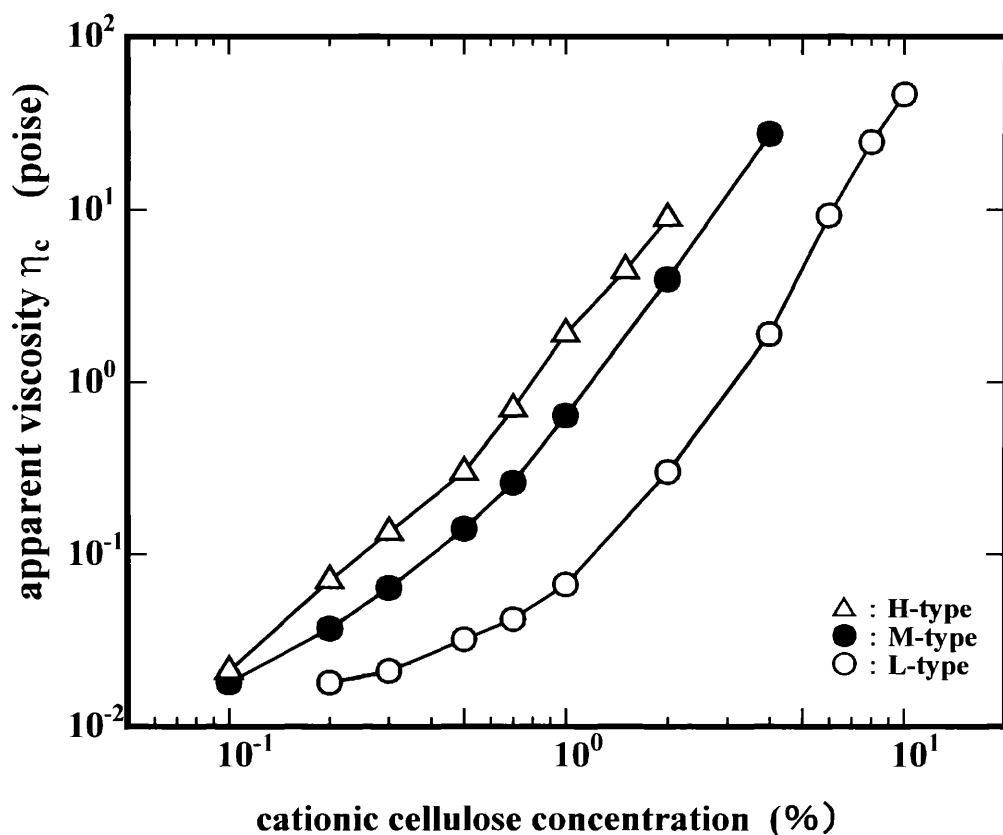


Figure 4. Relationship between apparent viscosity ( $\eta_c$ ) and cationic cellulose concentration.

aerosol foams. The experimental conditions were fixed at a maximum shear rate of  $320 \text{ sec}^{-1}$ , using a sweep time of 600 sec for the concentrates. A maximum shear rate of  $280 \text{ sec}^{-1}$ , using a sweep time of 200 sec, was used for the aerosol foams. Shear rate ( $d\gamma/dt$ ), shear stress ( $\tau$ ), and apparent viscosity ( $\eta$ ) were calculated on the basis of the Couette equation (22) for the concentric-cylinder setup and the Markovitz equation (23) for the cone-plate setup.

## RESULTS AND DISCUSSIONS

### GAS VOLUME FRACTION OF AEROSOL FOAM

The relation between the gas volume fraction of the aerosol foams,  $\phi$ , and the cationic cellulose concentration is shown in Figure 2. The gas volume fraction ( $\phi$ ) increases with the cationic cellulose concentration and becomes saturated near 0.96, regardless of the molecular weight. The critical concentration above which  $\phi$  levels off, on the other hand, increases with decreasing molecular weight.

### BUBBLE SIZE AND COALESCENCE RATE OF AEROSOL FOAM

The change in the average bubble size ( $D_N$ ) of the aerosol foams during aging is shown

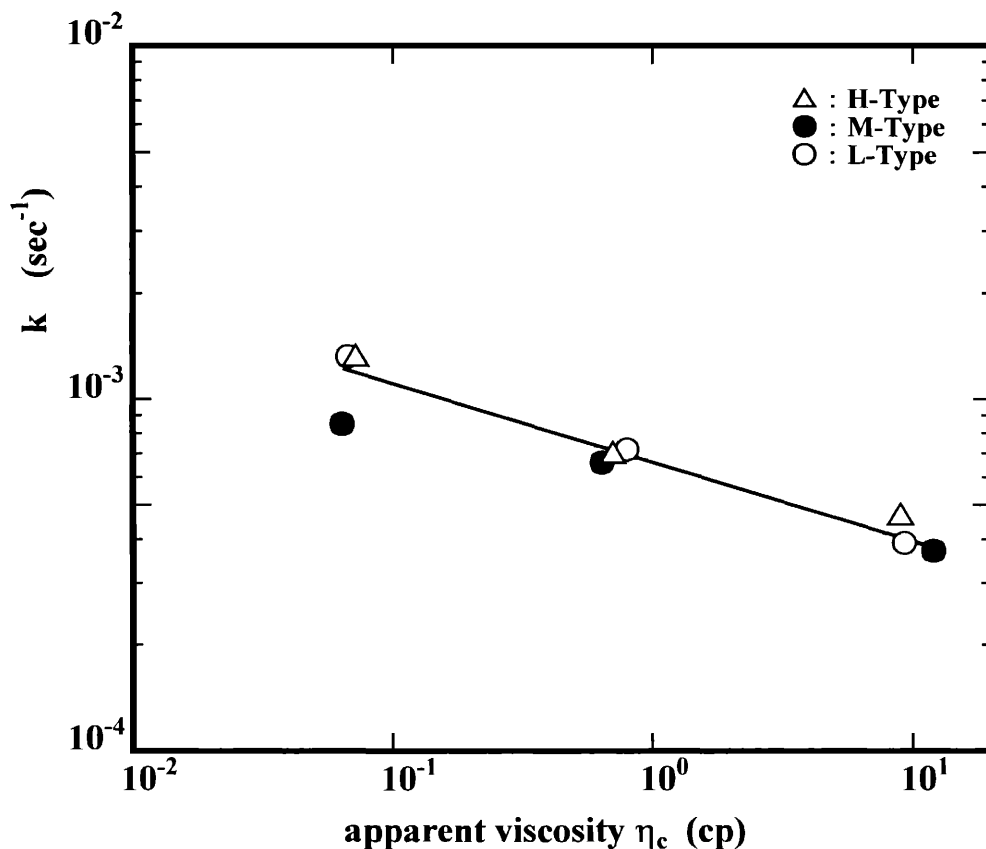


Figure 5. Relationship between apparent rate constant of coalescence ( $k$ ) and apparent viscosity ( $\eta_c$ ).

in Figure 3 for the M-type cellulose.  $D_N$  at all cationic cellulose concentrations shows a rapid increase followed by a more gradual increase.

The initial increase may be attributed to the volume expansion of evaporating the liquefied propellant. The average bubble size in the second stage increases linearly (Figure 3). It seems to be related to the first order kinetics of coalescence, expressed by equation 3:

$$\ln D_t = \ln D_0 + k \cdot t \quad (\text{Eq. 3})$$

where  $D_t$  is an average bubble size,  $D_0$  is the average bubble size at  $t = 0$ , and  $k$  is the apparent rate constant of coalescence. Values of  $D_0$  and  $k$  are summarized in Table I. For a given molecular weight,  $D_0$  remains constant regardless of concentration, while  $D_0$  decreases with increasing molecular weight. The apparent rate constant  $k$  defined in equation 3 decreases with increasing concentration of cationic cellulose.

#### RHEOLOGICAL PROPERTIES OF THE CONCENTRATE AND FOAM

*Apparent viscosity of the concentrate.* Figure 4 shows the relation between the cationic cellulose concentration and the apparent viscosity of the concentrate,  $\eta_c$ , at  $320 \text{ sec}^{-1}$ ;  $\eta_c$  increases with polymer concentration and molecular weight.

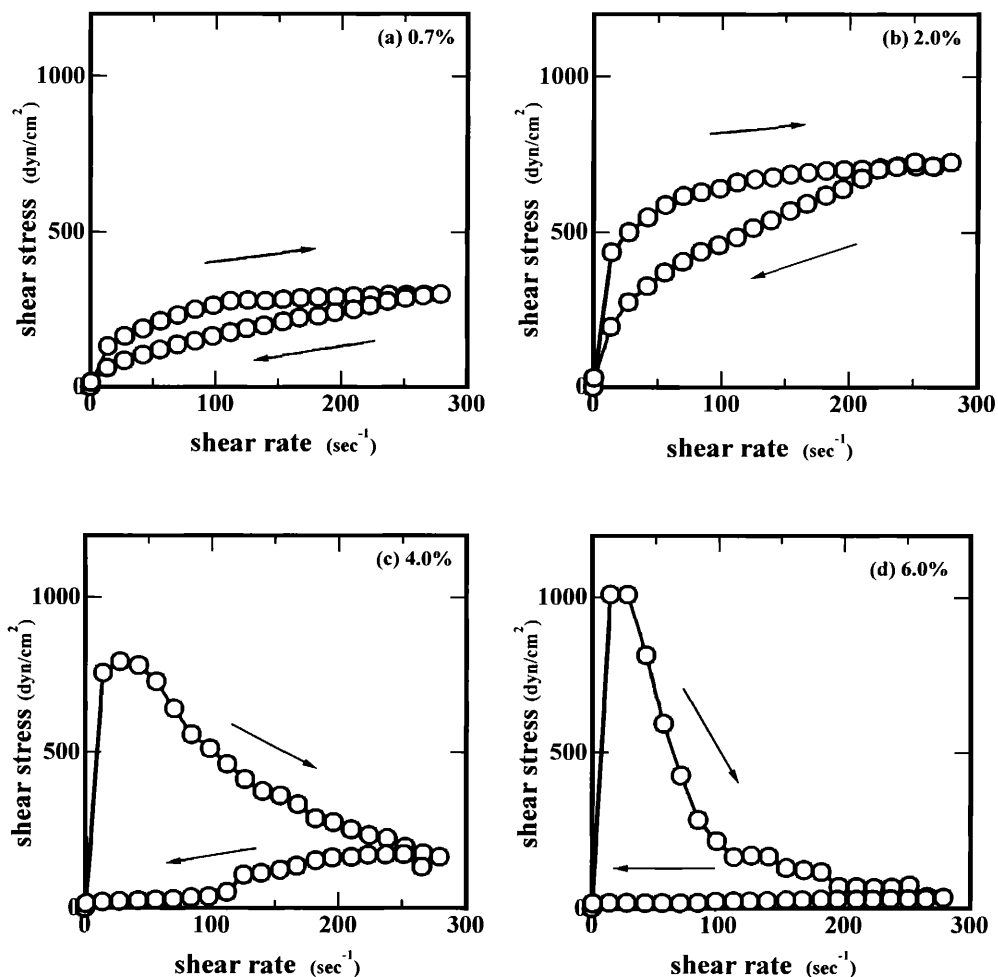


Figure 6. Flow curves of aerosol foam (L-type).

When the apparent rate constant,  $k$ , is plotted in a double logarithmic scale against  $\eta_c$ ,  $k$  decreases linearly, as shown in Figure 5, regardless of molecular weight, with increasing viscosity. Thus, the coalescence of the bubbles is uniquely determined by  $\eta_c$ .

*Flow curve for aerosol foam.* Flow curves for the L-type cationic cellulose in cyclic shearing tests are shown in Figure 6. When the cationic cellulose concentration is low, the flow curves for the aerosol foam show typical shear thinning flow with hysteresis (Figure 6a,b). The absolute value of the shear stress and the shear stress difference between the up and down curves increase with increasing cellulose concentration. Furthermore, the flow curves for higher cationic cellulose concentration show a typical spur on the up curve (Figure 6c,d). They differ from those of lower cationic cellulose concentration. This is a general tendency throughout the whole molecular weight regions.

*Yield value of aerosol foam.* From the flow curves exhibiting shear thinning (Figure 6a,b), Bingham yield values,  $\tau_B$ , were obtained. These values increase linearly with the cationic cellulose concentration on a log-log plot with a slope of about 0.8, as shown in Figure

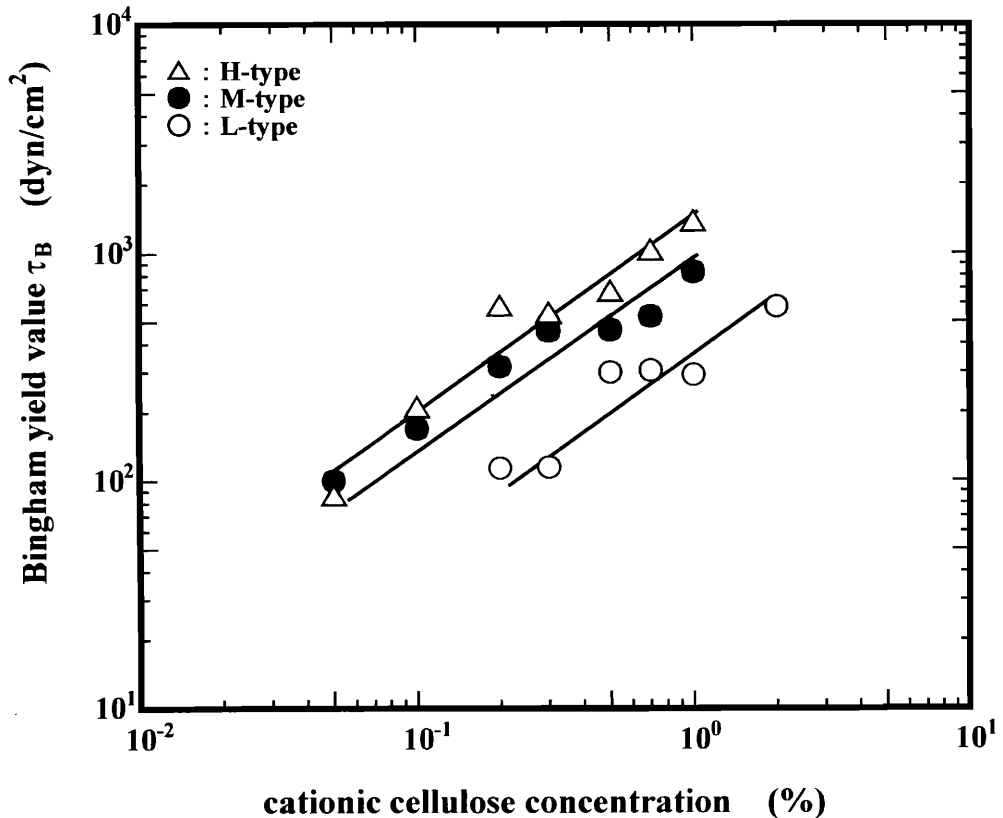


Figure 7. Relationship between Bingham yield value ( $\tau_B$ ) and cationic cellulose concentration.

7, for all the molecular weights of the cationic cellulose. For a given cationic cellulose concentration,  $\tau_B$  increases with the cationic cellulose's molecular weight. There is also a unique positive correlation between  $\tau_B$  and  $\eta_c$ , as shown in Figure 8, irrespective of the molecular weight, like the constant  $k$ . Therefore, both  $\tau_B$  and  $k$  seem to depend solely on the foam's stability.

*Apparent viscosity of aerosol foam at maximum shear rate.* The apparent viscosity,  $\eta_f$ , at a maximum shear rate of  $280 \text{ sec}^{-1}$  is plotted against  $\eta_c$  in Figure 9. A similar positive correlation was observed for  $\eta_f$  at the lower region of  $\eta_c$ . When  $\eta_c$  exceeds 0.3 poise, however,  $\eta_f$  tends to deviate from a straight line. The deviation takes place at a lower  $\eta_c$  when the molecular weight of the cationic cellulose is smaller.

#### DISSOLVED STATES OF THE COMPONENTS IN FOAMS

We now discuss the dissolved states of the components in foams on the basis of macroscopic flow behavior. Although the molecular weights of the cationic celluloses used in this study are different from each other, they all have 0.3–0.4 quaternary ammonium groups per anhydro-glucose unit. This means that one cationic substitution takes place per three glucose units on average. Acyl-glutamate is a dibasic acid. Since the average



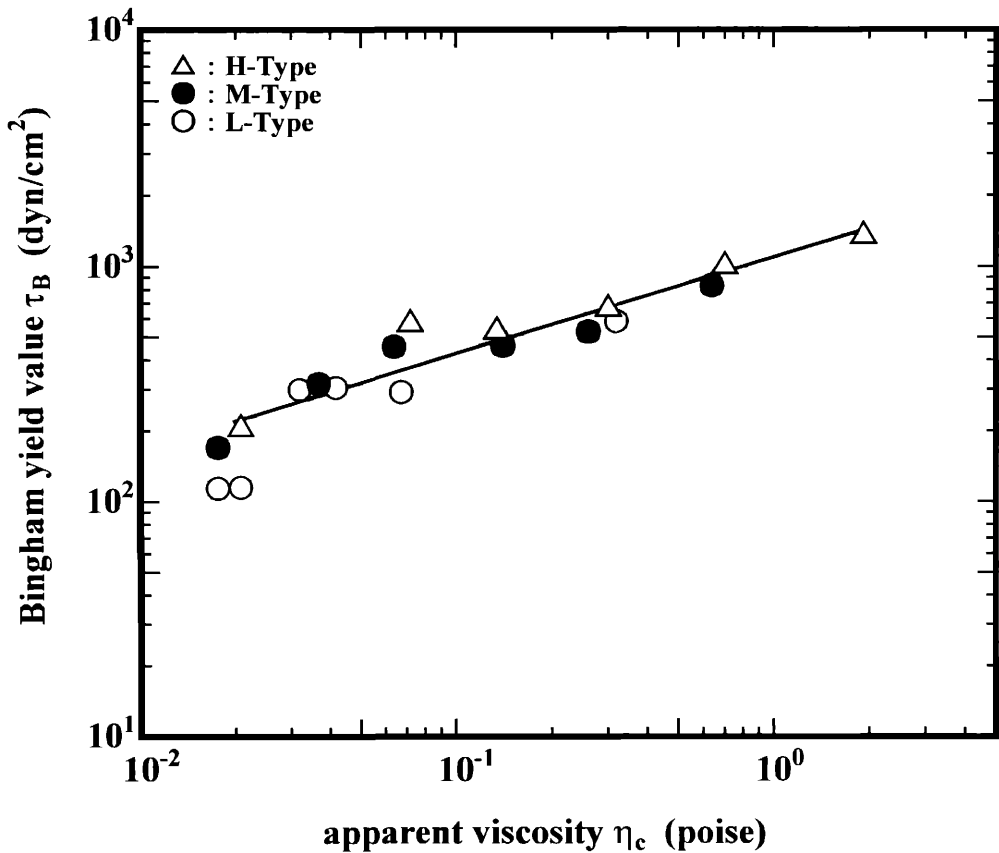


Figure 8. Relationship between Bingham yield value ( $\tau_B$ ) and apparent viscosity of the concentrate ( $\eta_c$ ).

degree of cationic substitution was about 0.3–0.4 per anhydro-glucose unit, one anionic surfactant molecule can be combined ionically to six glucose units on average. The weight ratio of the cationic cellulose to the anionic surfactant falls into 7/1, when they are at balance of the charge. The concentration of the anionic surfactant is 0.1 wt% in this study. We define the charge ratio of the cationic cellulose to the anionic surfactant as  $R$ . When  $R$  is unity, the concentration of cationic cellulose should be to 0.7 wt%.

Figure 10 expresses the results in Figure 9 in a different manner because the x-axis represents  $R$  instead of the cationic cellulose concentration. The maximum point on  $\eta_f$  is observed at a ratio,  $R$ , of *ca.* 2.0 between the cationic cellulose and the anionic surfactant for the M-type and the H-type, and *ca.* 4.0 for the L-type. Thus,  $\eta_f$  changed remarkably below and above  $R_{\max}$ , i.e., between 2.0 and 4.0.

Leung and Goddard (16) considered that the behavior of a solution comprising a cationic polymer (Polymer JR<sup>®</sup>) and sodium dodecyl sulfate was different as a function of the charge ratio between them. Maximal complex formation (precipitation) was observed near  $R$  of unity. As a consequence, the viscosity increases. Although the precipitation of the complex is low, a similar complex formation was recognized in a ternary component system with an additional nonionic surfactant (24,25).

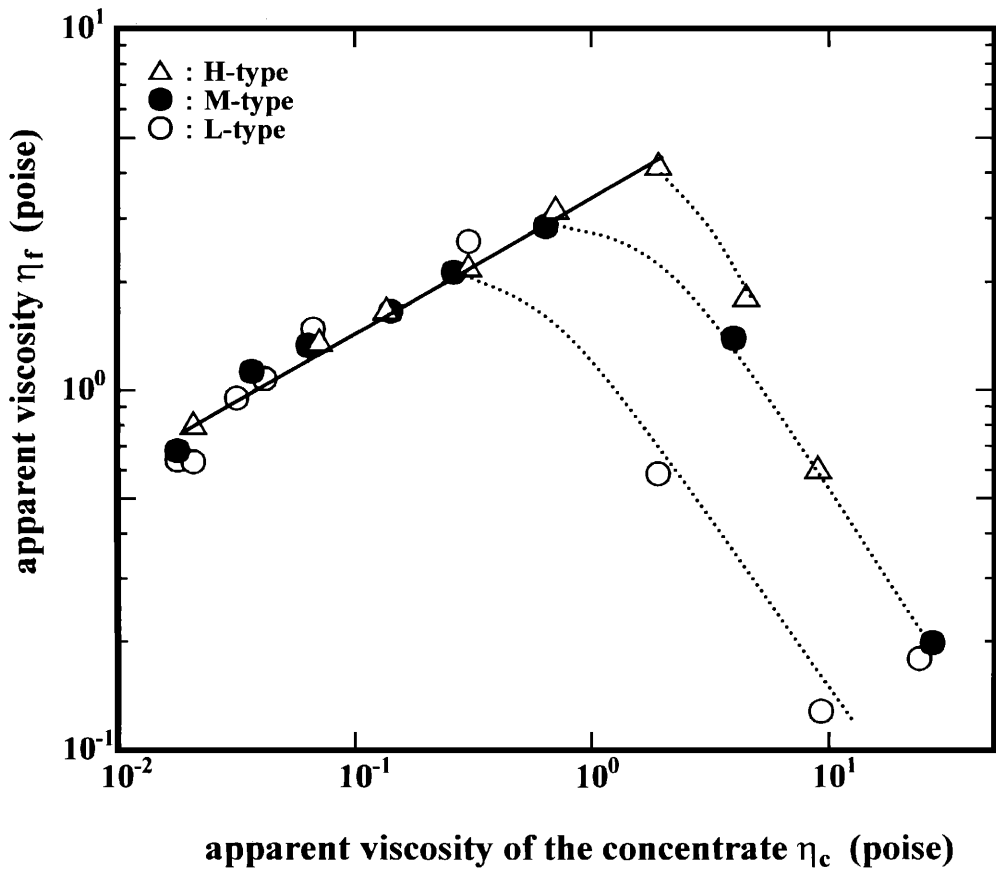


Figure 9. Relationship between apparent viscosity ( $\eta_f$ ) and apparent viscosity of the concentrate ( $\eta_c$ ).

From the foregoing we consider the dissolved state for the polymer and the surfactant in a liquid film of a foam as follows: When  $R$  is below  $R_{\max}$ , there exists the excess anionic surfactant, and the complex formation is increasing with the cationic cellulose concentration to  $R_{\max}$ , i.e., 2.0–4.0. Consequently, the thixotropic behavior is enhanced. Furthermore,  $\tau_B$  and thixotropy increase continuously, even when  $R$  exceeds  $R_{\max}$ . This could be explained by assuming increasing levels of entangled free cationic cellulose. When the shear rate is increased, however, the degree of entanglement among the charged cellulose chains decreases so that the desorption of the complexes at the air/liquid interface might occur. The interface between air and liquid then becomes unstable, resulting in the coalescence and the breakdown of the foams.

## CONCLUSIONS

The yield value,  $\tau_B$ , of the aerosol foams increases with the apparent viscosity of the concentrate,  $\eta_c$ . However, the apparent viscosity of the foams,  $\eta_f$ , shows a maximum value when plotted against  $\eta_c$ . The charge ratio between the cationic cellulose and the anionic surfactant,  $R$ , is 2.0–4.0 at the maximum  $\eta_f$ . From these results, we presume

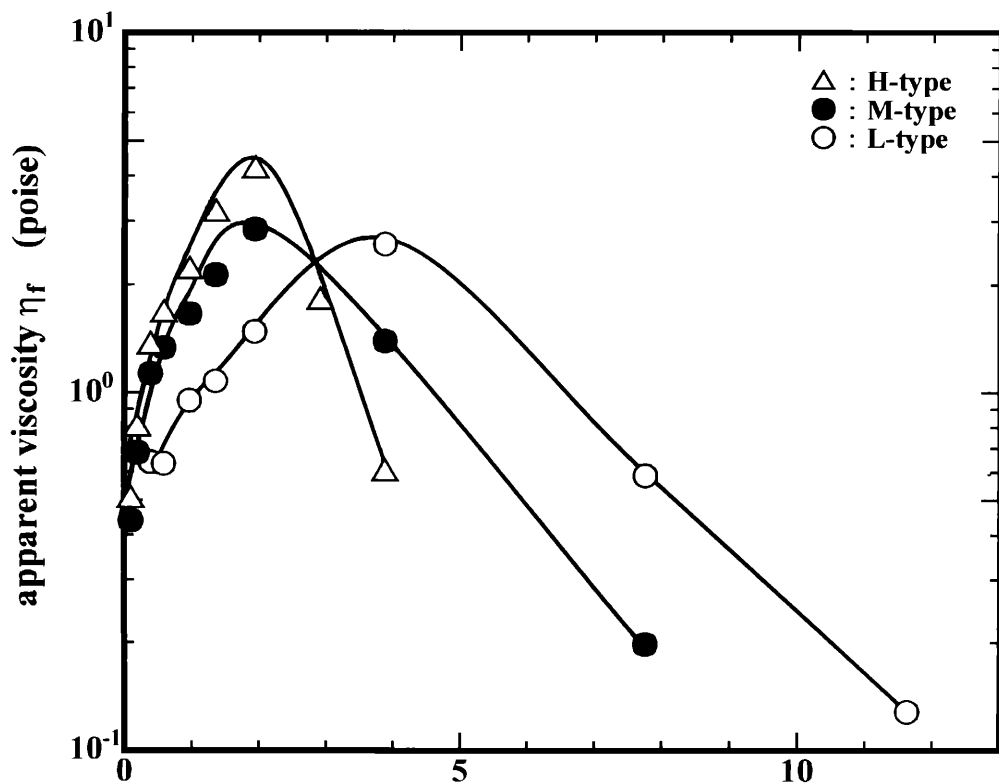


Figure 10. Relationship between apparent viscosity ( $\eta_f$ ) and charge number ratio (R).

that the dissolved state for the polymer and the surfactant in a liquid film of a foam is different below and above  $R_{\max}$ .

#### ACKNOWLEDGMENT

The author thanks Dr. Senna of the Faculty of Science and Technology of Keio University for many helpful suggestions during the course of this work.

#### REFERENCES

- (1) T. Tamura, The test methods for measuring foaming and antifoaming properties of liquid, *J. Jpn. Oil Chem. Soc.*, **42**, 737–745 (1993).
- (2) P. A. Sanders, *Handbook of Aerosol Technology*, 2nd ed. (Van Nostrand Reinhold, New York).
- (3) P. A. Sanders, Surfactants for aerosol foams, *Soap Chem. Spec.*, **39**, 63–67 (1963).
- (4) D. S. H. Sita Ram Sarma, J. Pandit, and K. C. Khilar, Enhancement of stability of aqueous foams by addition of water-soluble polymers—Measurements and analysis, *J. Colloid Interface Sci.*, **124**, 339–348 (1988).
- (5) P. A. Sanders, Molecular complex formation in aerosol emulsions and foams, *J. Soc. Cosmet. Chem.*, **17**, 801–830 (1966).
- (6) E. D. Goddard and P. S. Leung, Studies of gel formation, phase behavior and surface tension in mixtures of a hydrophobically modified cationic cellulose polymer and surfactant, *Colloids Surfaces*, **65**, 211–219 (1992).

- (7) P. S. Leung and E. D. Goddard, Gels from dilute polymer/surfactant solutions, *Langmuir*, **7**, 608–609 (1991).
- (8) E. D. Goddard, Polymer–surfactant interaction. Part I. Uncharged water-soluble polymers and charged surfactants, *Colloids Surfaces*, **19**, 255–300 (1986).
- (9) M. Nakagaki and S. Shimabayashi, Interaction of sodium dodecyl sulfate with poly(N-vinylpyrrolidone) and poly(vinyl alcohol) in aqueous solutions, *Nippon Kagaku Kaishi*, 1496–1502 (1972).
- (10) J. C. Brackman, Sodium dodecyl sulfate induced enhancement of the viscosity and viscoelasticity of aqueous solutions of poly(ethylene oxide). A rheological study on polymer-micelle interaction, *Langmuir*, **7**, 469–472 (1991).
- (11) N. A. P. Zugenmaier, Formation of supermolecular structures of polysaccharide-surfactant complexes in aqueous solutions. Influence of the polymer backbone, *Makromol. Chem.*, **194**, 1583–1593 (1993).
- (12) E. D. Goddard, T. S. Phillips, and R. B. Hannan, Water soluble polymer–surfactant interaction. Part I. *J. Soc. Cosmet. Chem.*, **26**, 461–475 (1975).
- (13) E. D. Goddard, R. B. Hannan, and G. H. Matteson, Dye solubilization by a cationic polymer/anionic surfactant system, *J. Colloid Interface Sci.*, **60**, 214–215 (1977).
- (14) E. D. Goddard and R. B. Hannan, Cationic polymer/anionic surfactant interaction, *J. Colloid Interface Sci.*, **55**, 73–79 (1976).
- (15) E. D. Goddard and R. B. Hannan, Polymer/surfactant interactions, *J. Am. Oil Chem. Soc.*, **54**, 561–566 (1977).
- (16) P. S. Leung and E. D. Goddard, A study of polycation-anionic-surfactant systems, *Colloids Surfaces*, **13**, 47–62 (1985).
- (17) K. P. Ananthapadmanabhan, P. S. Leung, and E. D. Goddard, Fluorescence and solubilization studies of polymer-surfactant systems, *Colloids Surfaces*, **13**, 63–72 (1985).
- (18) K. P. Ananthapadmanabhan, G.-Z. Mao, E. D. Goddard, and M. Tirrell, Surface forces measurements on a cationic polymer in the presence of an anionic surfactant, *Colloids Surfaces*, **61**, 167–174 (1991).
- (19) E. D. Goddard and P. S. Leung, in *Microdomains in Polymer Solutions*, P. L. Dubin, Ed. (Plenum Press, New York, 1985), pp. 407–415.
- (20) K. Ohbu, O. Hiraishi, and I. Kashiwa, Effect of quaternary ammonium substitution of hydroxyethylcellulose on binding of dodecyl sulfate, *J. Am. Oil Chem. Soc.*, **59**, 108–112 (1982).
- (21) K. Ohbu and S. Toyoda, Structural effects on the complex forming processes between water-soluble polymer and surfactant, *Hyomen*, **22**, 130–137 (1984).
- (22) M. M. Couette, Etudes sur le frottement des liquides, *Ann. Chim. Phys.*, **21**, 433–510 (1890).
- (23) H. Markovitz, L. J. Elyash, F. J. Padden, Jr., and T. W. DeWitt, A cone-and-plate viscometer, *J. Colloid Sci.*, **10**, 165–173 (1956).
- (24) P. L. Dubin and R. Oteri, Association of polyelectrolytes with oppositely charged mixed micelles, *J. Colloid Interface Sci.*, **95**, 453–461 (1983).
- (25) P. L. Dubin and D. D. Davis, Quasi-elastic light scattering of polyelectrolyte-micelle complexes, *Macromolecules*, **17**, 1294–1296 (1984).